Microelectronic Engineering 98 (2012) 19–23

Contents lists available at SciVerse ScienceDirect

Microelectronic Engineering

journal homepage: www.elsevier.com/locate/mee

The experimental investigation on dark current for InGaAs–InP avalanche photodiodes

Yanli Zhao [a,*], Suxiang He [b]

[a] Wuhan National Laboratory for Optoelectronics, School of Optoelectronics Science and Engineering, Huazhong University of Science and Technology, Wuhan 430074, China
[b] School of Science, Wuhan University of Technology, Wuhan 430070, China

ARTICLE INFO

Article history:
Received 20 February 2012
Received in revised form 6 May 2012
Accepted 2 June 2012
Available online 13 June 2012

Keywords:
Avalanche photodiodes (APDs)
Dark current
Noise

ABSTRACT

To meet the requirement of photon-starved detection, separate absorption grading charge multiplication avalanche photodiodes (SAGCM APDs) have drawn more and more attentions. In this work, we presents a detailed analysis of dark currents for planar-type SAGCM InGaAs–InP APDs with different sub-micron thicknesses of multiplication layer, considering the effect of the diffusion process, generation-recombination process and tunneling process. According to our knowledge, it is the first time clearly demonstrating that the dominant component of dark current for a SAGCM APD changes with multiplication gain from surface to volume contribution. Our finding could be beneficial to the optimization of an APD with a SAGCM structure. An optimal InGaAs–InP APD with low-voltage operation (<40 V) in combination with ultra-low dark current (0.10 nA@M = 8) has been demonstrated.

1. Introduction

The performance of the separate absorption grading charge multiplication avalanche photodiodes (SAGCM APDs) is strongly influenced by the thickness of the multiplication layer (X_d) [1,2]. As APDs are operated at low optical power levels, the noise is mainly originated from dark current. This dark current was found to increase with the increase of applied bias, thereby limiting the device performance. An important concern is that the increased dark current value constrains the useful gain of the APD to a low value. It is therefore of importance to optimize the internal electric field distribution of SAGCM APDs for dark current reduction. In this work, APDs with different thickness of multiplication layer were fabricated, and the device-level analysis of dark current for the planar-type SAGCM InGaAs–InP APDs has been presented. The effects of the diffusion process, generation-recombination process, and tunneling process were included during dark current analysis. An optimal InGaAs–InP APD with low-voltage operation (<40 V) in combination with ultra-low dark current (0.10 nA@M = 8) is reported. Considering the effective active surface area (50 μm in diameter) of APD, the dark current density is deduced to be as low as the 0.05 A/m^2. According to our knowledge, it is the first time to demonstrate that the dominant component of dark current for a SAGCM APD changes with multiplication gain from surface to volume contribution. Our finding could be beneficial to the optimization of the APD structure.

2. Experiments

The APD wafer epitaxial structure was grown in a single reactor growth cycle using metal organic chemical vapor deposition (MOCVD) process. The 2.0 μm thick undoped InGaAs layer is the absorption layer where the primary photo-generated carriers are generated. The generated electrons are swept by electric field to the n-contact, and generated holes travel to the undoped InP multiplication layer, i.e. nearly pure injection of photo-generated holes into the gain region is obtained, which gives the most advantageous structure for low-noise operation. The n^+-InP charge sheet layer is highly doped to decrease the electric field in the absorption layer. The undoped InGaAsP with graded composition was inserted to avoid hole accumulation in heterointerface between InP charge layer and the InGaAs absorption layer, i.e. the InGaAsP layer was used to match the energy band gaps of materials in multiplication and absorption layers. An effective active surface area is 50 μm in diameter, above which is coated with an antireflection SiNx layer. The MOCVD diffusion process has been adopted using Dimethylzinc (DMZn) as Zn source. Two-step diffusion process has been used for edge pre-breakdown suppression in our experiments. The diameter of the larger Zn diffusion active region window is 70-μm, while the diameter of the smaller Zn diffusion window is 50-μm. A two-dimensional scan of all the Zn diffusion region with a well-focused (<10 μm) spot of light was performed to assess the degree of non-uniformity in the response of the whole active region, and the results suggest that the edge pre-breakdown suppression has been successfully realized. Three APDs named samples I, II, and III were prepared in our experiments. The only

* Corresponding author. Tel.: +86 27 87792242; fax: +86 27 87792225.
E-mail addresses: wtdzhaoyl@163.com, yanlizhao@mail.hust.edu.cn (Y. Zhao).

0167-9317/$ - see front matter © 2012 Elsevier B.V. All rights reserved.
http://dx.doi.org/10.1016/j.mee.2012.06.001

Table 1
Structured parameters of the APD epitaxial structure.

Layer	Thickness (μm)	Doping (cm^{-3})
InP (p^+ diffusion layer)	3.0, 3.15 and 3.20 for samples I–III respectively	3×10^{18}
InP (multiplication layer)	0.5, 0.35 and 0.3 for samples I–III respectively	Un-doped
InP (charge)	0.3	1.10×10^{17}
GaInAsP (grading)	0.12	Un-doped
n-InGaAs (absorption)	2.0	Un-doped
n + InP (buffer)	1.0	1.0×10^{17}
n + InP substrates	100.0	1.0×10^{18}

difference among samples I–III is the different values of X_d. More details of the structural parameters of the fabricated APDs are tabulated in Table 1.

For dc photocurrent measurements, light with a wavelength of 1.31 μm and optical power of 0.1 μW was generated and transmitted over a monomode optical fiber to APD. A negative biased voltage in the range of 0 to $-V_{bd}$ (breakdown voltage) was provided to APDs with a step of −0.2 V, and the currents flowing through APDs during the change of voltage with and without light incidence were recorded automatically using a program-controlled Keithley voltmeter for dark and photo-current measurements, respectively. For SAGCM APD, it is a difficult and critical task to determine the unity gain (M_0). In this work, the determination of M_0 involves external quantum efficiency measurement. We utilize the standardized external quantum efficiency testing system in use of phase sensitive detection (PSD). By comparing the measured external quantum efficiency of the APD under test with a reference PIN photodiode that has the same thickness of the absorption layer as that of samples I–III, the APD gain at various bias voltages could be therefore estimated. After runs of measurements, it is concluded that the estimated error of this method can be controlled within 10%

3. Results and discussion

The measured dark current (total dark current, I_{dT}) of APDs can be viewed empirically as the superposition of two main current components, i.e. the surface current component and the bulk current component [3]. In an ideal APD, the I_{dT} can be expressed as a function of the multiplication factor M.

$$I_{dT} = I_{dM} \times M + I_{d0}, \tag{1}$$

where $I_{dM} \times M$ and I_{d0} denote multiplied and unmultiplied dark current, respectively. The $I_{dM} \times M$ is a volume contribution coming from the p-n junction central region. It is produced by generated carriers that flow through the p–n junction where the electric field is high enough to initiate impact ionization. The unmultiplied dark current I_{d0} is identified as a combination of surface contribution as well as the contribution from the peripherical edge of the active region of the planar APDs, where the electric field is lower than the central region of the pn junction and the multiplication is not expected to be built due to the suppression of edge pre-breakdown with the two-step Zn diffusion.

In theory, I_{dT} can be also quantitatively described by the sum of the three independent current sources: generation recombination of electron–hole pairs via traps in the depletion region (I_{gr}), tunneling of carriers across the bandgap (I_{tun}), and the diffusion current due to thermally generated minority carriers diffusing into the depletion region (I_{diff}) [4]. In our analysis, the tunneling via Shockley–Read-Hall (*SRH*) centers located within the bandgap was ignored since the measurement in our work is performed under relatively low reverse bias at room temperature [5]. For the sake of simplicity, the shunt current was also neglected. The theoretical components of the reverse dark current were therefore proposed as below [6,7].

$$I_{gr} \doteq (qn_iAw/\tau_{eff})[1 - \exp(-qV/2kT)], \tag{2}$$

$$I_{tun} \doteq \gamma A \exp(-\theta m_0^{1/2} \varepsilon_g^{3/2}/q\hbar E_m), \tag{3}$$

$$I_{diff} = I_S \cdot [1 - \exp(-qV/kT)], \tag{4}$$

where q is electronic charge, n_i is the intrinsic carrier concentration, A is the area of the active region, w is the depletion region width, τ_{eff} is the effective carrier lifetime, V is applied voltage, k is Boltzmann's constant, and T is the temperature in Kelvin. In Eq. (3), m_0 is the free-electron mass, E_m is the maximum junction electric field, $\hbar$ is Planck's constant divided by 2π, and ε_g is the energy gap. The γ and θ are explained in [6] in detail. In Eq. (4), I_s is the saturation current.

In a SAGCM APD, punch-through (*PT*) of the depletion region from InP multiplication region into the charge layer, grading layer, InGaAs absorption layer and highly doped InP buffer-layer occurs with the increase of the bias. A $p^+\nu$-APD is defined which consists of a highly doped p^+-InP layer forming an abrupt, one-sided junction with an intrinsic absorption ν (or n) layer of InGaAs. When the APD is biased with a voltage higher than a critical value (V_{diff}) above which the depletion region expands away from InGaAs layer to the InP buffer layer, it is defined that the APD works under the *PT* configuration. In this work, a detailed analysis of dark currents has been performed on planar-type SAGCM InGaAs–InP APDs considering the diffusion process, generation-recombination process, tunneling process, and multiplication process. Figs. 1–3 show the change of I_{dT}, I_L (photo-induced current) and M with bias for samples I, II and III, respectively. From Figs. 1–3, a series of values of critical voltage have been defined as V_{on}, $V_{M=8}$ and V_{br}. Among them V_{br} is the breakdown voltage of an APD, which can be

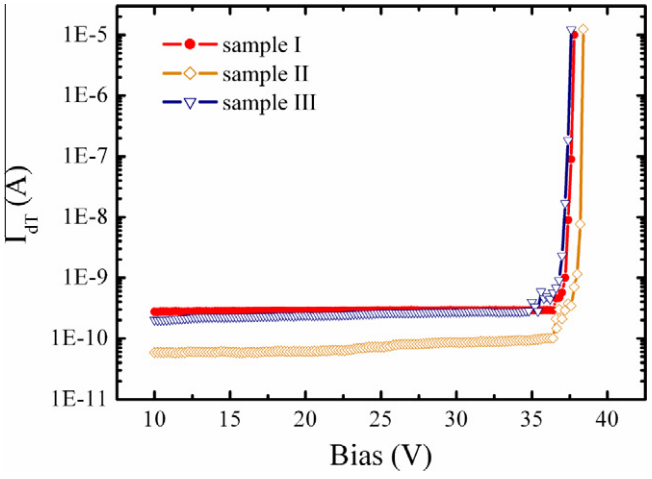

Fig. 1. The change of the measured dark current I_{dT} with bias for samples I, II, and III.

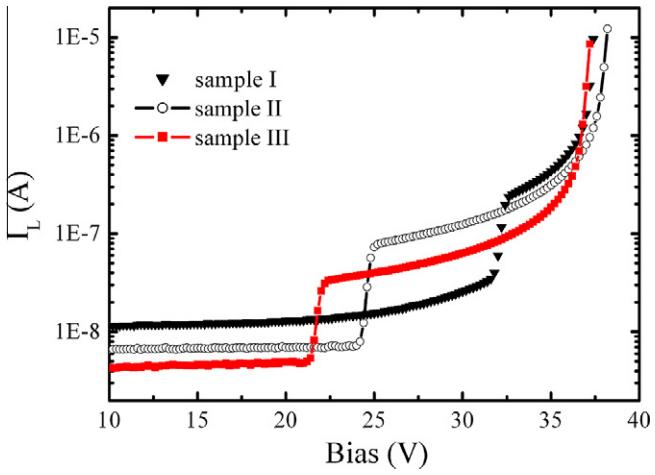

Fig. 2. The change of photo-induced current I_L with bias for samples I, II, and III.

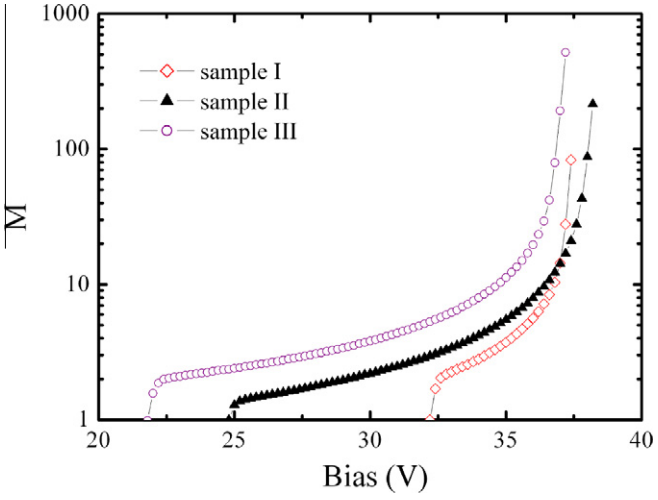

Fig. 3. The change of M with bias for samples I, II, and III.

deduced from Fig. 1 or Fig. 2. V_{on} deduced from Fig. 2 denotes the critical voltage of onset of photo-response, and $V_{M=8}$ deduced from Fig. 3 denotes the voltage biased when M equals to 8 for different APDs.

In Fig. 1, it is shown that V_{br} for samples I–III is about 37.8, 38.4 and 37.6 V, respectively. The difference of V_{br} among the three APDs is within 1.0 V. Combination of Fig. 1 with Fig. 3 reveals that the total dark current at $M = 8$ I_{dT8} is 0.45 nA for sample I, 0.1 nA for sample II, and 0.28 nA for sample III. I_{dT8} for sample I and sample III is 4.5 and 2.8 times as high as that for sample II. V_{diff} is another important parameter for APD, which denotes the critical voltage of *PT*. V_{diff} can be calculated with a series of electric field equations [8], just setting the electric field value being zero at the interface of

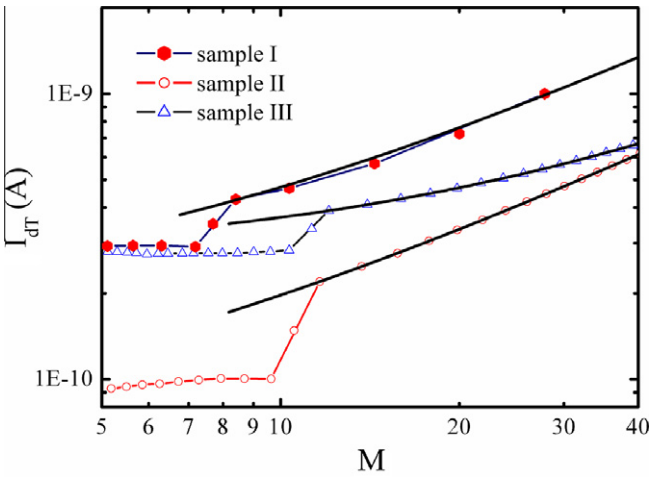

Fig. 4. The change of the measured dark current I_{dT} with M for samples I, II, and III, the solid lines denote the fit of the measurement with formula (1).

InGaAs absorption and InP buffer layer. The detailed parameters for I_{dT8}, V_{on}, V_{diff}, $V_{M=8}$ and V_{br} are also tabulated in Table 2.

For comparison, it is also tabulated in Table 2 the dark current density at 0.9 V_{br} (J_{dT}@0.9 V_{br}) for samples I–III from this work, as well as that for RefAPDI [9], RefAPDII [10], RefAPDIII [11] and RefAPDIV [12] reported from other groups. It is obvious that J_{dT}@0.9 V_{br} for Samples I–III from our work is much lower than that for their court parts from other groups, and the lowest J_{dT}@0.9 V_{br} of 0.05 A/m^2 is obtained in our work. In the absence of a clear, well-researched understanding of the suppression of dark current, it is conjectured that would be ascribed to the optimal device structure, and, to some degree, MOCVD diffusion and device passivation.

To shed light on the mechanism of the dark current suppression, the change of I_{dT} with M has also been studied, as shown in Fig. 4. The scattered data are from measurements, while the solid lines denote a linear fit of the measured dark current with Eq. (1). In the range of low M, the independence of I_{dT} on M reveals that I_{dT} is not dominated by I_{dM}. However, an abrupt increase of I_{dT} is observed with the increase of M. In combination with Fig. 3, the transition position of M and the corresponding bias for different APDs can thereby be deduced. Before the transition position, the independence of I_{dT} via M may indicate that the measured dark current is mainly dominated by I_{d0}. It is observed that I_{dT} increases linearly with M once M is larger than the transition value, which reflects that I_{dM} becomes the dominant component of dark current. I_{d0} and I_{dM} deduced from the linear fit with formula (1) have been summarized and tabulated in Table 2. For samples I, II to III, I_{d0} changes from 0.18, 0.059 to 0.269 nA, while I_{dM} changes from 0.029, 0.014 to 0.01 nA. Our results show that I_{dM} increases with the increase of the thickness of multiplication layer. It is stressed that the impact ionizations in the InP multiplication and charge layer may contribute to the multiplied dark current [8]. Moreover, due to the narrow bandgap, the contribution from impact ionization in the InGaAs absorption layer, and also InGaAsP grading layer

Table 2
The characteristic parameters of different APDs.

	I_{dT8} (nA)	V_{on} (V)	V_{diff} (V)	$V_{M=8}$ (V)	V_{br} (V)	I_{dM} (nA)	I_{d0} (nA)	J_{dT}@0.9 V_{br} (A/m^2)
Sample I	0.45	31.8	38.3	36.5	37.8	0.029	0.18	0.15
Sample II	0.10	24.0	29.6	36.0	38.4	0.014	0.059	0.05
Sample III	0.28	21.2	27.5	34.0	37.6	0.01	0.269	0.14
RefAPDI	–	–	–	–	–	–	–	31.85
RefAPDII	–	–	–	–	–	–	–	2.04
RefAPDIII	–	–	–	–	–	–	–	0.31
RefAPDIV	–	–	–	–	–	–	–	0.50

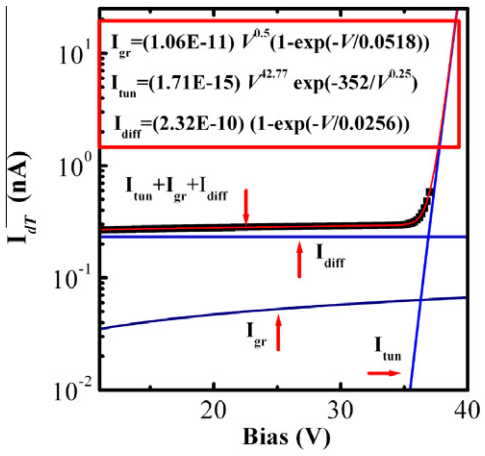

Fig. 5. The I_{dT} -*Bias* characteristic of sample I and the fit with the combination of I_{gr}, I_{tun} and I_{diff}.

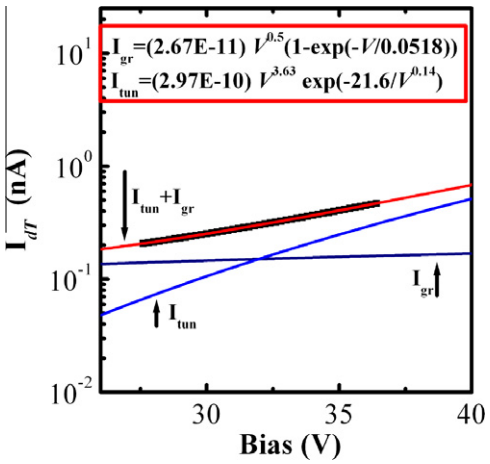

Fig. 7. The I_{dT}–Bias characteristic of sample III and the fit with the combination of I_{gr} and I_{tun}.

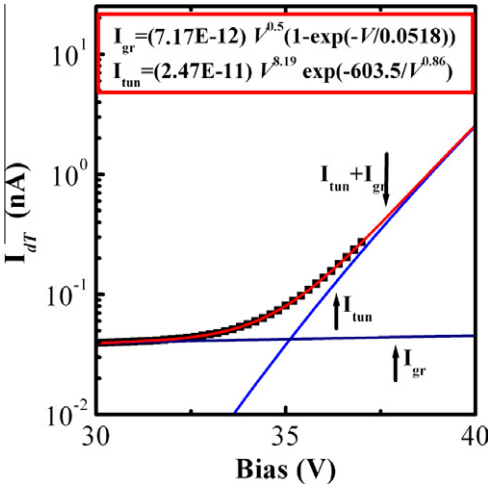

Fig. 6. The I_{dT} -*Bias* characteristic of sample II and the fit with the combination of I_{gr} and I_{tun}.

may be non-negligible [13]. The change in X_d alters the internal electric field distribution for SAGCM APDs, which may lead to the variation of impact ionization in different layers, and therefore the multiplied dark current changes. However, in contrast to I_{dM}, I_{d0} for sample II with the medium X_d is lower than that of its two counterparts. There is no doubt that the lowest I_{d0} contributes to the lowest I_{dT} for sample II. It is very interesting to found that the dominant component of dark current changes from I_{d0} to I_{dM} with an ideal linear behavior as M increases. In the following section, the underlying mechanism for dark current suppression in APDs is comprehensively investigated.

In Figs. 5–7, the dependence of I_{dT} on bias for samples I, II and III is shown, respectively. In Figs. 5–7, the scattered data denote the experimental work, while the solid lines denote the fit with formula (2)–(4). The theory and measurements are consistent with each other very well. For sample I, the calculated V_{diff} is about 38.3 V, which is even larger than V_{br} of the APD. As discussed above, the *PT* voltage was obtained from calculation of static field, not by measurements. The calculation is not very accurate since the dynamic carrier transport was neglected [14]. However, it is reasonable to predict that sample I is a $p^+\nu$-APD under the considered range of bias [7]. While for samples II and III, the calculated V_{diff} is about 29.6 and 27.5 V, both of which are much lower than their respective $V_{M=8}$. This means that samples II and III works under the *PT* configuration. The *PT* configuration is expected to be useful in reducing the total reverse-bias dark current when diffusion is a significant source of the leakage [7]. And therefore it is not difficult to understand that the diffusion current is shown to be the most important dark current component in sample I, while it seems to be of no significance in samples II and III.

The evidence for the prediction has been provided by the fit of measured dark current with formula (2)–(4), as shown in Fig. 5, which shows that the I_{dT} is indeed dominated by I_{diff} in the whole biased range. V_{diff} for samples II and III is 29.6 and 27.5 V, respectively, which is obviously lower than $V_{M=8}$ for each APD. Comparison of V_{diff} with $V_{M=8}$ reveals that the samples II and III are both with *PT* configuration. Figs. 6 and 7 show the measurement and the fit of dark current with combination of I_{tun} and I_{gr} for samples II and III, respectively. For the two APDs, it is found that the I_{diff} is two orders of magnitude smaller than I_{gr} and I_{tun} as we expected for *PT* APD and can be neglected. For sample II, I_{gr} is 0.043 nA, and I_{tun} is 0.091 nA, while for sample III, I_{gr} is 0.156 nA, and I_{tun} is 0.214 nA. Both I_{gr} and I_{tun} for sample II is smaller than that for sample III. The ratio of I_{gr} to $(I_{gr}+I_{tun})$ at $M=8$ has also been investigated for both of APDs. For samples II and III, the ratio of I_{gr} to $(I_{gr}+I_{tun})$ changes from 30% to 40%, which reveals the component of dark current can also be controlled by the change of the thickness of multiplication layer.

The structure of samples I, II and III is same except the thickness of multiplication layer. It is therefore to be expected that responsivity (quantum efficiency) is same for samples I–III due to the same thickness of absorption layer. For a fixed gain of 8, the dark current (I_{dT8}) decreases as the APD changs from $p^+\nu$ to *PT* configuration, as revealed by the comparison of sample I to sample II, as tabulated in Table 2. As the thickness of the multiplication layer further decreases, I_{dT8} increases again. This would be ascribed to the higher field applied on the InGaAs narrow bandgap layer for sample III than that for sample II. If it is reasonable to assume that the drift velocity of carriers for the *PT*-APDs (samples II and III) are with their saturation velocity due to the high electric field, the decrease of the multiplication layer thickness will improve the response speed. However, for sample I with $p^+\nu$ configuration, combination of the undepleted part of InGaAs layer and the thicker multiplication layer may slow down the response speed.

In summary, it is concluded that the punch-through configuration is beneficial to dark current reduction for SAGCM InGaAs–InP APDs in comparison with its $p^+\nu$ counterpart. The thickness of

multiplication layer should be optimized for the reduction of APD dark current. According to our knowledge, it is the first time to demonstrate that the dominant component of dark current for a SAGCM APD changes with M from I_{d0} to I_{dM}. The work is performed based on the InGaAs–InP materials, however, the methodology can be easily applied to other material systems, such as Ge–Si [15], InGaAs-InAlAs [16], III-Nitride [17], HgCdTe [18] and SiC [19,20] based-SAM APDs, which are widely used in optical communication, single-photon detection, infrared detection and violet detection and other fields.

4. Conclusions

In this work, we present a detailed analysis of dark currents for planar-type SAGCM InGaAs–InP APDs with different thicknesses of multiplication layer. It is suggested that optimization of the thicknesses of multiplication layer is an effective way for dark current reduction. Our work is performed based on the InGaAs–InP materials. However, the methodology would be applied to other material systems, such as Ge–Si, InGaAs-InAlAs, III-Nitride, HgCdTe and SiC based-SAM APDs. An optimal InGaAs–InP APD with low-voltage operation (<40 V) in combination with ultra-low dark current (0.10 nA@M = 8) has been demonstrated.

Acknowledgements

This work was supported by the National Hi-Tech Research and Development Program of China (No. 2008AA01Z207 and 2009AA03Z408), Natural Science Foundation of Hubei Province, China (No. 2010CDB01606), Research Funds for the Central Universities (Hust: No. 2011QN036), and Scientific Research Foundation for the Returned Overseas Chinese Scholars.

References

[1] S.G. Daniel Ong, M.M. Hayat, IEEE Photon. Technol. Lett. 23 (2011) 233.
[2] D.S.G. Ong, J.S. Ng, M.M. Hayat, P. Sun, J.P.R. David, J. Lightwave Technol. 27 (2009) 3294.
[3] K. Taguchi, T. Torikai, Y. Sugimoto, K. Makita, H. Ishihara, J. Lightwave Technol. 6 (1988) 1643.
[4] H.J. Song, C.H. Roh, J.H. Lee, H.G. Choi, D.H. Kim, J.H. Park, C. Hahn, Semicond. Sci. Technol. 24 (2009) 055012.
[5] W.D. Hu, X.S. Chen, F. Yin, Z.J. Quan, Z.H. Ye, X.N. Hu, Z.F. Li, W. Lu, J. Appl. phys. 105 (2009) 104502.
[6] S.R. Forrest, R.F. Leheny, R.E. Nahory, M.A. Pollack, Appl. Phys. Lett. 37 (1980) 322.
[7] S.R. Forrest, IEEE J. Quantum electronics 17 (1981) 217.
[8] Y. Zhao, S. He, Optics Commun. 265 (2006) 476.
[9] Kyung.-Sook. Hyun, Youngmi. Paek, Yong.-Hwan. Kwona, Ilgu. Yunb, El.-Hang. Lee, Proc. SPIE-Int. Soc. Opt. Eng. 4999 (2003) 130.
[10] Sungmin. Hwang, Jongin. Shim, Kyungyul. Yoo, J. Korean Phys. Soc. 49 (2006) 253.
[11] C.Y. Park, K.S. Hyun, S.K. Kang, M.K. Song, T.Y. Yoon, H.M. Kim, H.M. Park, S.-C. Park, Opt. Quantum Electron. 27 (1995) 553.
[12] Y. Liu, S.R. Forrest, V.S. Ban, K.M. Woodruff, J. Colosi, G.C. Erickson, M.J. Lange, G.H. Olsen, Appl. Phys. Lett. 53 (1988) 1311.
[13] J.S. Ng, C.H. Tan, J.P.R. David, G.J. Rees, IEEE J. Quantum Electron. 41 (2005) 1092.
[14] T. Kagawa, Y. Kawamura, H. Iwamura, Appl. Phys. Lett. 62 (1993) 1122.
[15] Y. Kang, M. Zadka, S. Litski, G. Sarid, M. Morse, M.J. Paniccia1, Y.-H. Kuo, J. Bowers, A. Beling, H.–D. Liu, D.C. McIntosh, J. Campbell, A. Pauchard, Opt. Express 16 (2008) 9365.
[16] J.C. Campbell, J. Lightwave Technol. 25 (2007) 109.
[17] C. Bayram, J.L. Pau, R. McClintock, M. Razeghi, Appl. Phys. Lett. 92 (2008) 241103.
[18] J. Beck, C. Wan, M. Kinch, J. Robinson, P. Mitra, R. Scritchfield, F. Ma, J. Campbell, J. Electron. Mater. 35 (2006) 1166.
[19] Q.G. Zhou, D. McIntosh, H.-D. Liu, J.C. Campbell, IEEE Photon. Technol. Lett. 23 (2011) 299.
[20] Q.G. Zhou, D.C. McIntosh, Z. Wen Lu, J.C. Campbell, A.V. Sampath, Appl. Phys. Lett. 99 (2011) 131110.